

OBSERVATION OF A PLASMA WAKEFIELD BUILD-UP CAUSED BY A TRAIN OF LINAC BUNCHES

A. OGATA¹, Y. YOSHIDA², N. YUGAMI⁴, K. MIYA², Y. NISHIDA⁴,
H. NAKANISHI¹, K. NAKAJIMA¹, S. TAGAWA³, H. SHIBATA³, T. KOZAWA²,
T. KOBAYASHI² and T. UEDA²

*National Laboratory for High Energy Physics, Tsukuba, 305 Japan¹
Nuclear Engineering Research Laboratory,*

*The University of Tokyo, Tokai-mura, Naka-gun, Ibaraki-ken, 319-11 Japan²
Research Center for Nuclear Science and Technology,*

*The University of Tokyo, Tokai-mura, Naka-gun, Ibaraki-ken, 319-11 Japan³
Department of Electrical and Electronic Engineering,
Utsunomiya University, Utsunomiya, 321 Japan⁴*

(Received 26 August 1991; in final form 7 November 1991)

The plasma wakefield caused by a train of linac bunches was detected using a coaxial diode detector. The idea of obtaining a high acceleration gradient in a plasma wakefield accelerator using a train of bunches is therefore examined. Each bunch had an identical amplitude, though the envelope had finite rise and fall times. It was shown that wave amplitude cannot grow infinitely, but reaches saturation. We calculated the wakefield at saturation from the experimentally-obtained damping time of the plasma wave using linear theory and found that it could be 400 times higher than that caused by a single bunch.

1 INTRODUCTION

A plasma wakefield accelerator (PWFA) is one of the plasma-based type accelerators that shows promise in producing ultra-high accelerating gradients. In the PWFA, a high-intensity relativistic driving bunch excites a large-amplitude plasma wave which, in turn, accelerates a low-intensity trailing bunch.¹ Our previous paper has reported an energy shift of more than 10 MeV in a 1 m long plasma in the PWFA.² The PWFA must attain a high transformer ratio in order to become a real accelerator, which is the ratio between the energy reached by the trailing bunch and that lost from the driving bunch. One of the methods proposed to attain a high ratio is to make a driving bunch with a triangular longitudinal particle distribution.³ Because this idea is technically difficult to realize, an alternative method is proposed which uses a train of driving bunches with a triangular envelope.^{4,5}

This paper reports on preparatory experiments concerning this bunch-train method. A train of identical bunches was introduced into a plasma, and the resultant high-frequency plasma wave was detected using a coaxial diode detector. The time

evolution of the plasma wave was compared with a calculation which took account of wave damping.

The next section describes calculations based on linear theory. Both computer simulations and analytical solutions which approximate the bunch train as a continuous cosine function are given. The experimental setup is given in Section 3. The experimental results are reported in Section 4. The last section contains discussion and conclusions.

2 CALCULATION

The wakefield E caused by an impulsive bunch is expressed by

$$\ddot{E} + 2\beta\dot{E} + \omega_p^2 E = E_0\delta, \quad (2.1)$$

with initial conditions $E(-0) = \dot{E}(-0) = 0$, where ω_p is the plasma frequency and β is the damping frequency of the plasma wave. Its solution is given by

$$\frac{E(t)}{E_0} = \exp(-\beta t)[\cos \omega_0 t - (\beta/\omega_0) \sin \omega_0 t], \quad (2.2)$$

where $\omega_0 = (\omega_p^2 - \beta^2)^{1/2}$. An estimation of E_0 depends on the physical model used. If we assume a transverse parabolic distribution with radius a , we have

$$E_0 = -\frac{4r_e m_e c^2 N}{a^2} \left[2K_2(ka) + 1 - \frac{4}{(ka)^2} \right], \quad (2.3)$$

on the beamline,⁶ where N denotes the number of electrons, k denotes the plasma wave number, and K is a modified Bessel function. The wakefield caused by a train of identical impulsive bunches is just a superposition of $E(t)$,

$$W(t) = E(t) + E(t - \tau) + E(t - 2\tau) + \cdots + E(t - n\tau) + \cdots, \quad (2.4)$$

where $E(t - n\tau) = 0$ if $t < n\tau$, and $\tau = 2\pi/\omega_l$ is the period of the linac bunches.

Figure 1 shows the calculated time evolution of the plasma wave for the case where the resonant condition $\omega_p = \omega_l$ is satisfied. If β is zero, the wave amplitude grows to infinity; if β is not zero, the wave saturates. The saturation occurs when the increase in the wakefield produced by a single bunch, $\Delta W = +E_0$, is equal to the decay between bunches, $\Delta W = -W\beta\tau$, giving $\lim_{n \rightarrow \infty} W(n\tau - 0) = E_0/\beta\tau$. As β becomes large, both the saturation level and the time to reach this value become small. Figure 2 shows the calculated evolution of a plasma wave for the case $\omega_p \neq \omega_l$. If β is zero, a steady beat-wave appears. If β is not zero, the wave amplitude reaches a certain constant level. This level becomes low as the difference $(\omega_p - \omega_l)$ becomes large, and/or β becomes large. The beat-wave characteristic appears transiently. The length of the transient is inversely-proportional to β .

Let us observe these figures on an expanded scale. Figure 3(a) shows a wakefield caused by the first of several linac bunches for the case where $\omega_p = \omega_l$ and $\beta = 0$. Each linac bunch gives a negative jump in the waveform, showing that the energy

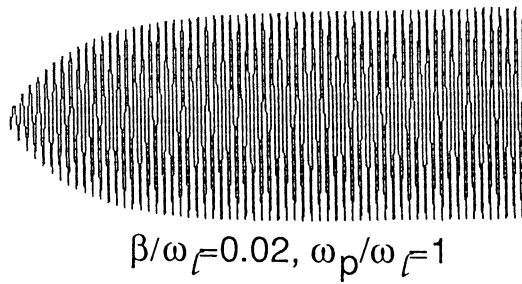
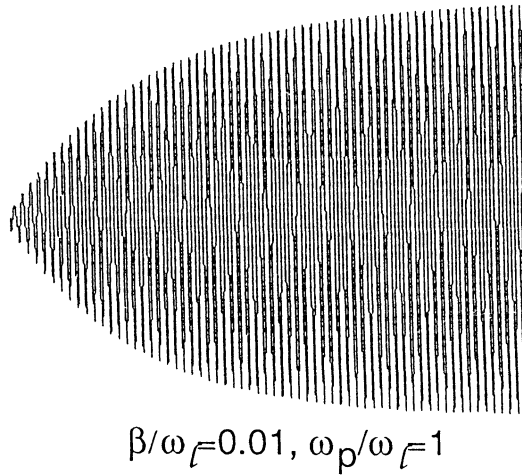
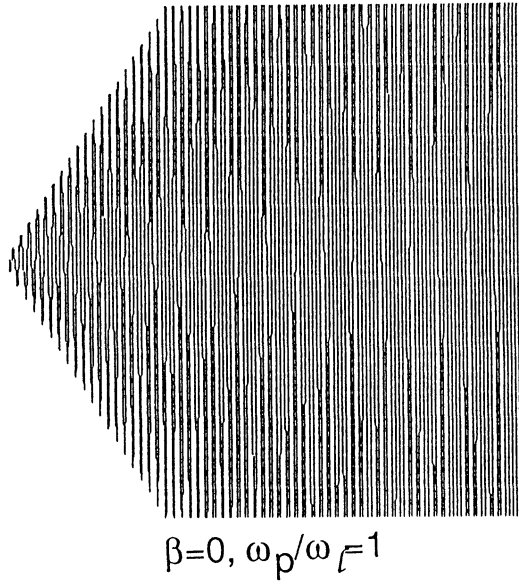


FIGURE 1 Evolution of a plasma wave with $\omega_p = \omega_L$. The response to the first 64 linac pulses is shown.

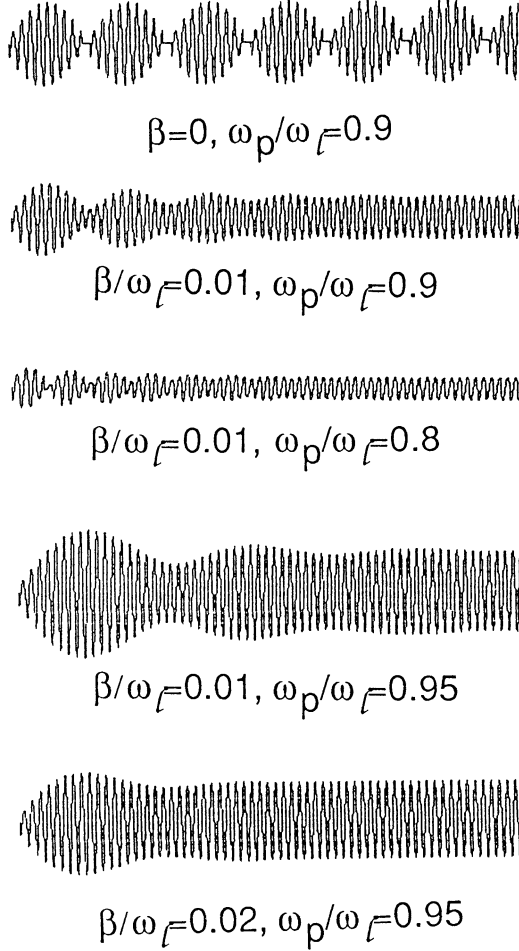


FIGURE 2 Evolution of a plasma wave with $\omega_p \neq \omega_l$. The response to the first 64 linac pulses is shown.

of the bunch is decelerated to raise the plasma wakefield. The amount of deceleration grows with time. Using an energy analyzer, we could observe an increasing negative energy shift of linac bunches. The figure indicates that we could accelerate a test bunch if it were injected at a time when the amplitude is positive. Figures 3(b)–(c) show another case, where ω_p does not coincide with ω_l and β is not zero. Figure 3(b) shows the response to the first several bunches while (c) shows the steady state. The beam energy, which is given by the vertical position after each negative jump in the figure, at first fluctuates, and then approaches a constant value.

This final amplitude can be analytically calculated as following. From Eqs. (2.2) and (2.4) we have

$$W(n\tau_{-0})/E_0 = \sum_n \exp(-n\beta\tau) [\cos n\omega_0\tau - (\beta/\omega_0) \sin n\omega_0\tau]. \quad (2.5)$$

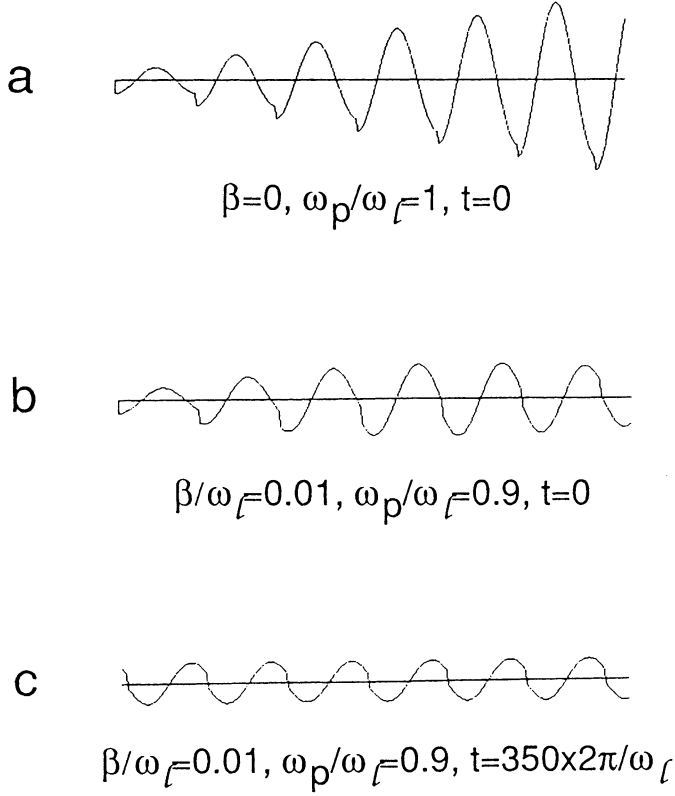


FIGURE 3 Evolution of a plasma wave in a magnified time scale.

The following equalities

$$\lim_{n \rightarrow \infty} \sum_n a^n \sin nx = \frac{a \sin x}{1 - 2a \cos x + a^2},$$

and

$$\lim_{n \rightarrow \infty} \sum_n a^n \cos nx = \frac{a \cos x - a^2}{1 - 2a \cos x + a^2},$$

yield

$$\lim_{n \rightarrow \infty} W(n\tau_{-0})/E_0 = \frac{\exp(-\beta\tau)[\cos \omega_0\tau - (\beta/\omega_0) \sin \omega_0\tau] - \exp(-2\beta\tau)}{1 - 2 \exp(-\beta\tau) \cos \omega_0\tau + \exp(-2\beta\tau)}. \quad (2.6)$$

If the resonant condition $\cos \omega_0\tau = 1$ is satisfied, it reduces to

$$\lim_{n \rightarrow \infty} W(n\tau_{-0})/E_0 = \frac{\exp(-\beta\tau)}{1 - \exp(-\beta\tau)} \sim \frac{1}{\beta\tau} = \frac{\omega_0}{2\pi\beta}. \quad (2.7)$$

We also have $\lim_{n \rightarrow \infty} W(n\tau_{+0})/E_0 \sim 1/(\beta\tau) + 1 \sim 1/\beta\tau$.

Aside from the microscopic behavior, the time evolution of the envelope of the plasma wave can be better described by an equation in which an approximation is applied regarding the bunch train as a cosine wave with a frequency equal to the bunch frequency. Since an actual bunch train envelope has a finite rise time of α , the following equation is useful when discussing the time evolution of the envelope of the plasma wave:

$$\ddot{W} + 2\beta\dot{W} + \omega_p^2 W = E_0 \omega_p^2 \cos \omega_i t [1 - \exp(-\alpha t)], \quad (2.8)$$

with initial conditions $W(0) = \dot{W}(0) = 0$. The solution is complicated. Using the approximation $\alpha \sim \beta \sim |\omega_p - \omega_i| \ll \omega_p, \omega_i$, we have

$$\begin{aligned} W(t)/(\omega_p^2 E_0) = & \exp(-\beta t) [A_r \cos(\omega_p^2 - \beta^2)^{1/2} t + B_r \sin(\omega_p^2 - \beta^2)^{1/2} t] \\ & + \exp(-\alpha t) [C_r \cos \omega_i t + D_r \sin \omega_i t] \\ & + [E_r \cos \omega_i t + F_r \sin \omega_i t], \end{aligned} \quad (2.9)$$

where

$$\begin{aligned} A_r &= \frac{\omega_i^2 - \omega_p^2}{G} - \frac{\omega_i^2 - \omega_p^2 + \alpha(2\beta - \alpha)}{H}, \\ B_r &= \frac{-1}{(\omega_p^2 - \beta^2)^{1/2}} \left[\frac{(\alpha - \beta)(\omega_p^2 + \omega_i^2) + O(\alpha^3)}{H} - \frac{(\omega_p^2 + \omega_i^2)\beta}{G} \right], \\ C_r &= \frac{\omega_i^2 - \omega_p^2 + \alpha(2\beta - \alpha)}{H}, \quad D_r = \frac{-2\omega_i^2(\beta - \alpha) + O(\alpha^3)}{\omega_i H}, \\ E_r &= (\omega_p^2 - \omega_i^2)/H, \quad F_r = 2\omega_i \omega_p / H, \quad G = (\omega_i^2 - \omega_p^2)^2 + 4\omega_i^2 \beta^2, \end{aligned}$$

and

$$H = (\omega_i^2 - \omega_p^2)^2 + 4\omega_i^2 \beta^2 + 2\alpha(\alpha - 2\beta)(\omega_i^2 + \omega_p^2).$$

Terms A_r, B_r, C_r and D_r give the transient response; terms E_r and F_r give the steady-state response, which can be arranged as

$$W(\infty)/E_0 = [(\omega_p^2 + \omega_i^2)/((\omega_i^2 - \omega_p^2)^2 + 4\omega_i^2 \beta^2)^{1/2}] \sin(\omega_i t + \theta), \quad (2.10)$$

where $\tan \theta = -(\omega_i^2 - \omega_p^2)/(2\omega_i \omega_p)$. If $\omega_p = \omega_i$, this equation reduces to $W(\infty)/E_0 = (\omega_i/\beta) \sin \omega_i t$. Because of the cosine envelope approximation, this equation differs from Eq. (2.7) by a factor of 2π , and ω_i replaces ω_0 .

A similar equation gives the response of a plasma to a beam with a finite fall time; *i.e.*,

$$\ddot{W} + 2\beta\dot{W} + \omega_p^2 W = E_0 \omega_p^2 \cos \omega_i t \exp(-\alpha t). \quad (2.11)$$

Let us consider that the linac current begins to fall after the stationary state has been established; in other words, the bunch envelope is sufficiently long to reach the steady-state wakefield as given in Eq. (2.10). The initial conditions then become $W(0) = E_0 \omega_p^2 / [(\omega_i^2 - \omega_p^2)^2 + 4\omega_i^2 \beta^2]^{1/2}$ and $\dot{W}(0) = 0$, if the initial point is the mo-

ment just after the linac pulse is fed. The solution of Eq. (2.11) then becomes

$$W(t)/(\omega_p^2 E_0) = \exp(-\beta t)[A_f \cos(\omega_p^2 - \beta^2)^{1/2} t + B_f \sin(\omega_p^2 - \beta^2)^{1/2} t] \\ + \exp(-\alpha t)[C_f \cos \omega_1 t + D_f \sin \omega_1 t], \quad (2.12)$$

where

$$A_f = \frac{1}{\sqrt{G}} + \frac{\omega_i^2 - \omega_p^2 + \alpha(2\beta - \alpha)}{H}, \\ B_f = \frac{1}{(\omega_p^2 - \beta^2)^{1/2}} \left[\frac{\beta}{\sqrt{G}} + \frac{(\alpha - \beta)(\omega_p^2 + \omega_i^2) + O(\alpha^3)}{H} \right], \\ C_f = \frac{\omega_p^2 - \omega_i^2 - \alpha(2\beta - \alpha)}{H},$$

and

$$D_f = \frac{2\omega_i^2(\beta - \alpha) + O(\alpha^3)}{\omega_1 H}.$$

3 EXPERIMENTAL SETUP

The experimental setup is similar to that used for plasma lens experiments.⁷ The experiments were conducted at the University of Tokyo on a 14 MeV linac,⁸ which produces a bunch train, each part of which has a rms length (measured by a streak camera) less than 3 mm, or 10 psec. The bunch frequency is 2.85 GHz, or the intra-bunch period is 350 psec; the duration of the bunch train is 6 μ sec, and the repetition rate of the train is 6.25 Hz. The maximum charge of a bunch in the present experiments was about 50 pC.

We usually separate the plasma chamber from the linac duct using metal foils in order to avoid any vacuum problems. One obstacle in this case is multiple scattering of the beam caused by the foils and gas along the beam transport, which decreases the charge density and the resultant plasma wakefield. By using differential pumping we solved this problem, thus enabling separation without having to use any hard boundaries. Four turbomolecular pumps were used, three of which were placed between the linac main duct and the plasma chamber. Ducts with low conductance, 16 mm in diameter and 1233 mm in total length, connected the linac and the plasma. An automatic gate valve was used to close the line whenever the pressure of this section exceeded the prescribed value.

An argon plasma was produced in the chamber (147 mm in inner diameter and 360 mm in length) by a discharge between the LaB₆ cathodes and the plasma chamber in synchronism with the linac bunch. The plasma pulse width was about 2 msec. It was confined by using the multidipole field of permanent magnets placed around the chamber periphery. The magnetic field had a maximum value of 700 G at the

chamber wall. One of the features of this type of confinement is that there is no magnetic field along the beam transport. The argon plasma density ranged from $0.5 - 15 \times 10^{10} \text{ cm}^{-3}$ and the temperature from 2.5–4 eV, as measured by a Langmuir probe. The measurement shows that the plasma length along the beam transport is about 15 cm for the case $n_e = 1.3 \times 10^{11} \text{ cm}^{-3}$, which increases to 20 cm for $n_e = 0.75 \times 10^{11} \text{ cm}^{-3}$. The electron density was controlled by either the discharge current or the gas flow.

The experiments were carried out using a plasma of around $n_e = 1.01 \times 10^{11} \text{ cm}^{-3}$, where the plasma frequency (ω_p) is equal to the linac bunch frequency (ω_l), and $T_e = 2 \text{ eV}$. The acceleration gradient caused by the wakefield of a single bunch of this linac would be approximately 4.07 keV/m according to Eq. (2.3), with $a = 3 \text{ mm}$. Without any damping, a bunch train of $6 \mu\text{sec}$ would build up the wakefield, resulting in a gradient of 23 MeV/m. This value is still below the wave-breaking amplitude E given by

$$eE/m\omega_p c = 1, \quad (3.1)$$

which is $\sim 30 \text{ MeV/m}$ in this plasma.

The oscillation power was measured by a KC-2 coaxial diode detector produced by Nihon Koshuha Co., with a frequency response that sharply cuts off at 3 GHz. As shown in Figure 4(a), the diode was connected between a semi-rigid cable and the Langmuir probe. The probe was inserted perpendicular to the plasma, the end of which was 1 cm off-center from the beamline. The dc component of the signal was short-circuited to the ground by a BNC-T connector in order to protect the detector. A $\pi/2$ bending magnet was placed downstream of the plasma as an energy analyser. The half width of the linac beam energy measured by this method was approximately 5%, or 700 keV.

4 EXPERIMENTAL RESULTS

Figure 4(b) shows a typical pair of envelope waveforms: those of the beam current and the power of the plasma oscillation. Note that the waveform of the plasma wave shown in Figure 4(b) should be compared with the square of the envelope of the oscillations shown in Figures 1–3. Figure 5 gives two examples of plasma oscillation envelopes with different amplitudes.

The five main results obtained are: 1) As long as the oscillation amplitude is small, the envelope of the plasma oscillation power is almost rectangular, similar to the linac bunch train envelope (Figure 4). 2) When the amplitude exceeds 1 V, the envelope of the plasma oscillation has an irregular shape (Figure 5), often revealing a low frequency component. 3) The amplitude of the plasma oscillation is sensitive to the plasma density around the resonance ($\omega_p = \omega_l$). 4) The rise and fall times are, however, independent of the plasma density, when the amplitude is less than 1 V. 5) No difference was observed between the energy spectre measured with and without the resonant plasma.

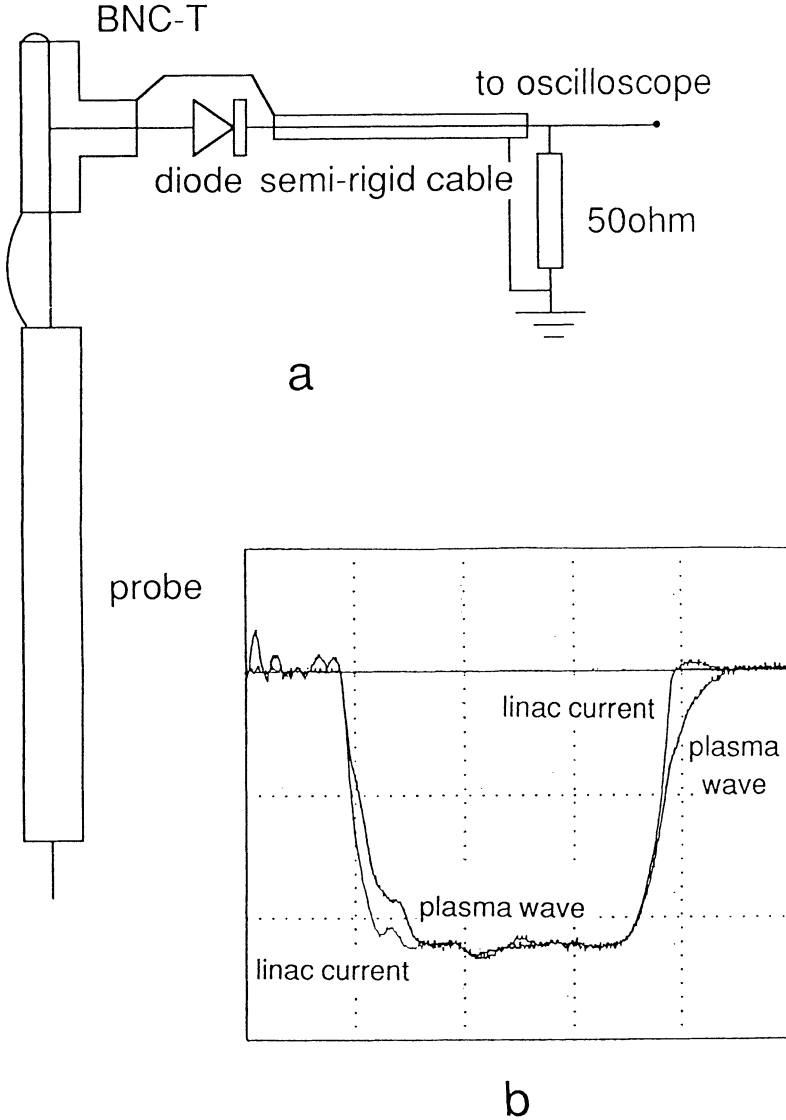


FIGURE 4 (a) Setup for plasma oscillation detection. (b) Envelopes of the linac beam current and the plasma oscillation. The horizontal scale is $2 \mu\text{sec/div.}$, and the vertical scale is arbitrary.

Results 1) and 2) show the existence of wave damping. Results 3) and 4) are consistent with those of the previous analysis, which tells us that, once the time structure of the bunch train is given, the rise and fall times of the plasma oscillation envelope are determined only by the damping frequency (β). To the contrary, not only β but also $\omega_p - \omega_l$, the difference between the plasma frequency and the linac pulse frequency, contribute to the saturation level, as shown in Eq. (2.10). Result 5)

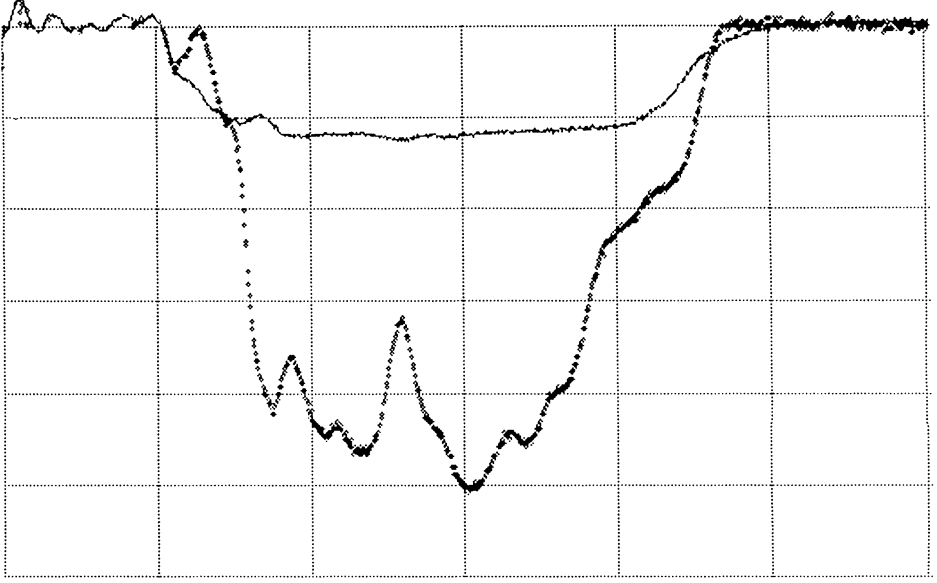


FIGURE 5 Envelopes of the plasma oscillation with different amplitudes. The horizontal scale is $2 \mu\text{sec}/\text{div.}$ and the vertical scale is $0.25 \text{ V}/\text{div.}$

was obtained because the maximum-possible energy change caused by the 20 cm long plasma is less than the resolution of the energy analyzer, 700 keV. We will discuss this result later.

Result 2) must be due to the density fluctuation. As shown by Eq. (2.10), the amplitude grows large when $(\omega_l - \omega_p)/\omega_l \ll 1$, and becomes sensitive to $\omega_l - \omega_p$, which is, of course, a function of the plasma density. In this situation, a small density fluctuation is magnified and appears as a fluctuation of the envelope. Another explanation is that the difference $(\omega_p - \omega_l)$ appeared as a beat with a low frequency of around 600 kHz in Figure 5.

If the amplitude of a plasma wave envelope on an oscilloscope is less than 1 V, we can derive the damping frequency of the plasma wave (β) from the waveforms. An example of the oscilloscope traces of the plasma oscillation is shown in Figure 4 together with that of the linac current. Equations (2.8) and (2.11) give the macroscopic response of the wakefield when the linac bunch envelope has a finite rise time of $1/\alpha_r$ or a finite falltime of $1/\alpha_f$. From the curve showing the linac current envelope in Figure 4(b), we have $\alpha_r = 3.00 \text{ MHz}$ and $\alpha_f = 1.10 \text{ MHz}$. We first take the square roots of the data showing a rise in the plasma wave envelopes, and fit the results to

$$A_r = \exp(-\beta t)\sqrt{A_r^2 + B_r^2} + \exp(-\alpha t)\sqrt{C_r^2 + D_r^2} + \sqrt{E_r^2 + F_r^2}, \quad (4.1)$$

to obtain β . In the case of a fall in the plasma wave envelopes, we fit the results to

$$A_f = \exp(-\beta t)\sqrt{A_f^2 + B_f^2} + \exp(-\alpha t)\sqrt{C_f^2 + D_f^2}. \quad (4.2)$$

Using the Marquardt method, a nonlinear least-square fit algorithm, we have for a rise $\beta = 470 \pm 81$ kHz and for a fall $\beta = 1.20 \pm 0.05$ MHz. The standard deviations are calculated from 20 values. If we regard this system as a resonator, the quality factor becomes $Q = \omega_p/\beta = 5185 \sim 7344$ for a rise and $Q = \omega_p/\beta = 2280 \sim 2484$ for a fall. The falling section gives better statistics. One reason for this is because

$$\frac{\sqrt{A_r^2 + B_r^2}}{\sqrt{C_r^2 + D_r^2}} < \frac{\sqrt{A_f^2 + B_f^2}}{\sqrt{C_f^2 + D_f^2}}, \quad (4.3)$$

which can be understood after carefully comparing Eqs. (2.9) and (2.12). Another reason is because the time dependence at the falling section is smoother than at the rising section, as shown in Figure 4(b). Since the data concerning the falling section is more reliable, a further consideration regarding these data is made.

Using this experimental value, we find that the steady state amplitude could amount to $W(\infty)/E_0 = \omega_p/(2\pi\beta) \sim 400$ (Eq. (2.7)). This is quite a large magnification, which gives a gradient of 1.6 MeV/m. The actual energy shift in these experiments with a 20 cm long plasma is less than 320 keV, which is difficult to detect using an energy analyzer with poor resolution. This is the reason for result 5) itemized at the beginning of this section.

5 DISCUSSION AND CONCLUSIONS

Three subjects are discussed here. First is the signal amplitude caught by the diode detector, second is the effect of the plasma density fluctuation and third is the wave damping mechanism.

First, let us check consistency between the wakefield amplitude and the signal amplitude detected by the diode. Because the probe is inserted perpendicular to the beamline, we consider that the probe is sensitive only to the radial component of the wakefield. The maximum amplitude of the radial wakefield caused by a single linac bunch is given by⁶

$$E(r) = \frac{8r_e mc^2 N}{a^2} I_2(ka) K_0(kr), \quad r > a \quad (5.1)$$

which is 19.5 V/m at $r = 10$ mm. Multiplying it by the probe length, 1 mm, we have the voltage across the probe $V = 19.5$ mV. The power felt by the diode is $V^2/R = 7.63 \mu\text{W}$ with $R = 50 \Omega$. Since the diode has a sensitivity of ~ 1 mV/ μW , the voltage caused by a single linac pulse is ~ 7.63 mV. The maximum amplitude we observed, temporarily, was ~ 2 V, which is the result of the buildup of $2 \text{ V}/7.63 \text{ mV} = 262$ linac bunches. The calculation tells us that, at the optimum, we could build up 400 linac bunches. This rough estimation of signal amplitude agrees fairly well with the calculation. However, we could not stably maintain this maximum amplitude in the experiments, as shown in Figure 5. The maximum stable amplitude was ~ 1 V, which is equivalent to the buildup of 131 linac bunches. The energy shift

caused by the buildup of 131 bunches in a 20 cm long plasma is 104 keV, which is not detectable using an energy analyzer with a resolution of only 700 keV.

The difficulty in maintaining the maximum wave amplitude suggests that plasma density fluctuation hinders the buildup in the density region around the resonance. Because Q was ~ 2000 in the present experiments, the plasma density must be controlled within an accuracy of $1/(2 \times 2000) \sim 0.025\%$ throughout the buildup period of the plasma wakefield, 400 intra-bunch periods in the present case, if we aim at the maximum amplitude. (The derivative of Eq. (2.10) with respect to ω_p would give more direct analysis on the sensitivity of the wakefield amplitude to the density fluctuation.) The fluctuation imposes a severe limit on the length of a bunch train when we apply the present method in the real field. Some feedback mechanism is necessary which tracks and tunes the plasma density to the resonance. Equation (2.10) implies another fact; the existence of damping weakens the wakefield, but it eases the effect of density fluctuation.

The fluctuation has little effect in the density region near to the resonance. This fact gave good reproducibility to the damping frequency measurement, $\beta = 1.20 \pm 0.5$ MHz for 20 values. What mechanism then caused the damping of the plasma wave in the present experiments? Landau damping in the longitudinal direction is negligibly small, since the phase velocity of the plasma wave is equal to the velocity of the linac beams; *i.e.*, the light velocity. The possibility of Landau damping in the transverse direction will be discussed elsewhere.⁹ One possible mechanism is collisional damping. The electron-electron and electron-ion collision frequencies¹⁰ in the present case become respectively

$$v_{ee} = 5 \times 10^{-6} n_e (\text{cm}^{-3}) \ln \Lambda / T_e (\text{eV})^{3/2} = 962 \text{ kHz},$$

$$v_{ie} = 2 \times 10^{-6} Z n_e (\text{cm}^{-3}) \ln \Lambda / T_e (\text{eV})^{3/2} = 384 \text{ kHz}.$$

The summation is quite close to the experimental value. Because the plasma is not fully ionized, collisions between electrons and neutral atoms also contribute to the damping, though they are not so effective as the above collisions.

In conclusion, the present experiments show that a Langmuir probe combined to a coaxial diode detector gives qualitative information concerning the plasma wakefield. They tell us that we must take into account both the damping of the plasma wave and the plasma density fluctuation in order to attain acceleration using a bunch train. Because of the damping and the density fluctuation, growth of the wakefield produced by a train of bunches with identical amplitudes is limited. However, if the plasma density were optimized, the steady state amplitude could amount to $W(\infty)/E_0 = \omega_p/(2\pi\beta) \sim 400$, or a gradient of 1.6 MeV/m even in the present experiments.

REFERENCES

1. P. Chen, J. M. Dawson, R. W. Huff and T. Katsouleas, *Phys. Rev. Lett.* **54**, 693 (1985).
2. A. Enomoto, H. Kobayashi, K. Nakajima, H. Nakanishi, Y. Nishida, A. Ogata, S. Ohsawa, T. Oogoe, Y. Suetsugu and T. Urano, *Proc. 2nd. European Part. Accel. Conf.* (Nice, 1990) Editions Frontieres, Gif-sur-Yvette, 1991, vol. 1, p. 634.
3. K. L. F. Bane, P. Chen and P. B. Wilson, *IEEE Trans. Nucl. Sci.* **NS-32**, 3254 (1985).

4. K. Nakajima, *Part. Accel.* **32**, 209 (1990).
5. B. Zotter, *CERN CLIC Note* 18 (1986).
6. R. D. Ruth, A. W. Chao, P. L. Morton and P. B. Wilson, *Part. Accel.* **17**, 171 (1985).
7. H. Nakanishi, Y. Yoshida, T. Ueda, T. Kozawa, H. Shibata, K. Nakajima, T. Kurihara, N. Yugami, Y. Nishida, T. Kobayashi, A. Enomoto, T. Oogoe, H. Kobayashi, B. S. Newberger, S. Tagawa, K. Miya and A. Ogata, *Phys. Rev. Lett.* **66**, 1870 (1991).
8. H. Kobayashi and Y. Tabata, *Nucl. Instr. and Meth.* **B10/11**, 1004 (1985).
9. A. Ogata, Y. Yoshida, N. Yugami, Y. Nishida, H. Nakanishi, K. Nakajima, S. Tagawa, H. Shibata, T. Kozawa, T. Kobayashi and T. Ueda, *Bull. Am. Phys. Soc.* **36**, 2364 (1991).
10. F. F. Chen, "Introduction to Plasma Physics and Controlled Fusion", 2nd. ed. (Plenum Press, New York, 1985), vol. 1.